Evolution in Electrical and Electronic Engineering Vol. 4 No. 2 (2023) 544-551

EEEE

Homepage: http://publisher.uthm.edu.my/periodicals/index.php/eeee
e-ISSN : 2756-8458

Dual Rotor PMFSM for Counter-Rotating Wind Turbine

Mohd Hanif Lutpi[1], Mahyuzie Jenal[1]*

[1]Faculty of Electrical and Electronic Engineering,
University Tun Hussein Onn Malaysia, Batu Pahat, 86400, MALAYSIA

*Corresponding Author Designation

DOI: https://doi.org/10.30880/eeee.2023.04.02.067
Received 30 January 2023; Accepted 04 July 2023; Available online 30 October 2023

Abstract: A wind turbine consists of a turbine rotor installed for wind rotation that has many blades that convert the energy in the wind into rotational energy. Wind turbines consist of two sets of counter-rotating rotors leading to twice the power density. Flux Switching Machine (FSM) is one of the new categories of electric motors developed by previous researchers and has become popular for electrical AC motor applications. Permanent Magnetic Flux Switch Machine (PMFSM), Field Excitation Flux Switch (FEFSM), and Hybrid Excitation Flux Switch are the three types of FSM (HEFSM). One of these is PMFSM, which offers advantages such as low cost, simple construction, and FEC-free winding that obtains minimal copper loss—suitable for diverse performances. This work presents a design study and investigative analysis of a PMFSM twin rotor with rotor poles for counter-rotating wind turbines. Diverse permanent magnet flux switching range devices are available in terms of design (PMFSM). PMFSM with segmented permanent magnet PM consequent pole arrangement, on the other hand, is intensively researched. Moreover, PMFSM is examined with several rotor positions, including inner and exterior rotors. To achieve motor performance in terms of torque, power, and speed, a dual rotor arrangement with varied stator configurations is used. Dual rotors have been a popular issue in the field of electrical machine research because they offer a twin-rotor configuration to boost output torque and power. Yet, when torque and power increased, other motor characteristics, such as back-EMF, worsened, resulting in higher-order harmonic content. Finally, at the end of this chapter, all of the findings from the research will be summarized.

Keywords: Dual Rotor PMFSM, Wind Turbine

1. Introduction

This study examines the rotor pole combinations for a counter-rotating wind turbine's permanent magnet flux switching machine (PMFSM). Renewable energy sources including wind, solar, and biomass have attracted a lot of interest recently. The need for energy grows along with improved living circumstances and societal advancement. A global economic figure called energy consumption per

Corresponding author: mahyuzie@uthm.edu.my

capita rises because of increased electric energy use. By 2040, the demand for energy is expected to be 25% more than it is today. Large- and small-scale wind power generation has recently been used for several purposes [1]. Malaysia is renowned for having an area with a moderate wind speed in compared to other nations. Because Malaysia's average yearly wind speed is less than 2 m/s, most wind turbines require a minimum wind speed of 4 m/s to produce power. As a result, wind energy has yet to be adequately captured in Malaysia.

Permanent magnet flux switching machines (PMFSM) are frequently described in the literature in terms of the nature of the flux and the position of the rotor. Alternative stator constructions and dual rotor positions (inner rotor and outer rotor) were also investigated to increase power density in stator permanent magnet machines. Because of the accessible interior area, internal rotor topologies of permanent magnet flux switching generators (PMFSG) allow the direct coupling of turbine blades with rotors with more poles [2]-[4]. The inner rotor area of a dual-rotor PMFSM is underutilized in order to increase power density or voltage output. Furthermore, the concept of counter-rotation is applied to a variety of generating topologies for higher power density.

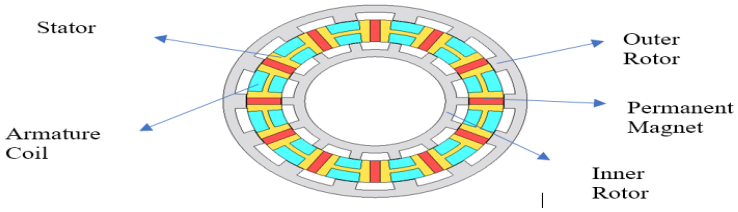

Figure 1: Design Dual Rotor PMFSM

2. Materials and Methods

The core functionality of JMAG-Designer mostly pertains to the processes of geometry drawing, and model setup, including material utilized, condition setting, circuit, study magnetic, run analysis, mesh, and result graph plotting. JMAG Designer has also made research easier from a time and money perspective because simulation results are trustworthy and attainable. Additionally, JMAG Designer accurately detects and evaluates complicated physical phenomena inside the machine.

2.1 Materials and Conditions

Table 1 tabulates the components and conditions used while configuring the rotor, stator, armature coil, and permanent magnet, with the rotor's durable rotational speed set to 500 r/min. Furthermore, the nodal force is applied to the rotating axis in an upward direction. The reason for this is that the torque that operates on magnetic materials must be specified and calculated.

Table 1: List of specific materials and condition

Parts	Materials	Condition
Rotor	Nippon Steel 35H210	Motion: Rotation Torque: nodal force
Stator	Nippon Steel 35H210	-
Armature Coil	Conductor Copper	FEM Coil
Permanent Magnet	Neomax35AH (irreversible)	Motion: Rotation Torque: nodal force

(Alternate Radial and
Circumferential Anisotropic
Pattern)

2.2 Investigation of Operating for Dual Rotor PMFSM

In general, this study is divided into two sections, particularly the JMAG-designer and the geometry editorial manager. Every component of the machine, such as the stator, rotor, armature coil, and FEC, must be calculated independently using Geometry Editorial Manager, while JMAG-Designer is required for condition settings and simulation. Coil test analysis was done in both the inner and outer rotors at no load to establish the functioning principle of dual Rotor PMFSM. Figure 2 depicts the flowchart for the coil test analysis in JMAG-Designer and the geometry editor.

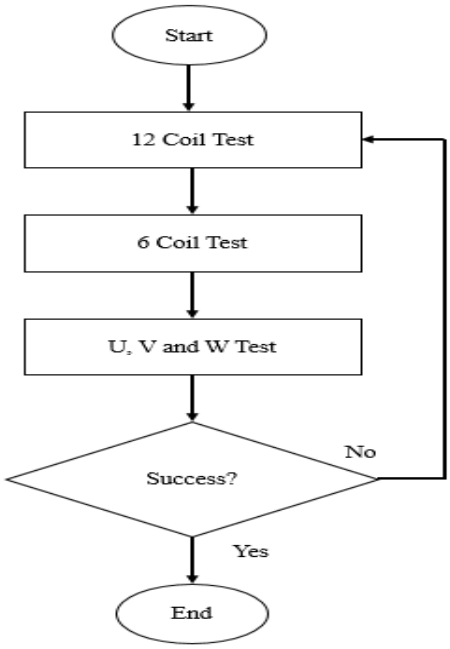

Figure 2: The coil test analysis workflow

The machine's performance in terms of back-emf, cogging torque, flux lines, and flux distribution is noted in the no-load study after the coil test analysis. The load analysis is performed by supplying the armature coil's current density, Ja. The pattern is discovered by studying torque and flux correlations at various Ja areas. of torque change when different current levels are fed into the motor's FEM coil. The armature current density varies from 0 to 30 (A/mm2) during the load test. As shown in Equation 1, the number of turns on the armature coil is calculated using the same technique as the armature coil input current value.

$$I_a = \frac{J_a \alpha S_a}{N_a} \quad (Eq.1)$$

Where,

Ia = Input current of the armature coil A/mm^2

Ja = Armature coil current density

$\alpha a = Armature\ coil\ filing\ factor$

Sa = Armature coil slot area

Na = Number of turns of the armature coil

$$fe = Nrfm \quad (Eq. 2)$$

$fe =$ Electrical frequency

Nr = Number of poles

$fm =$ Mechanical frequency

Table 2 tabulates the input current of the armature coil.

Table 2: 12S-14P Double Rotor PMFSM Input current of the armature coil

Armature coil current density, JA (A/mm2)	Input current of armature coil, IA (A)	Input current of armature coil, Arms (A)
0	0	0
5	11.1459	7.8813
10	22.2917	15.7626
15	33.4376	23.6439
20	44.5834	31.5252
25	55.7293	39.4065
30	66.8751	47.2878

To determine the maximum torque, output power, and motor speed, a torque and power versus speed study was performed (rpm). Eq. 3, which is based on the torque versus speed curve, is used to calculate the motor's output power.

$$P_o = \frac{2\pi N_M \tau}{60} \quad (Eq. 3)$$

where

N_M = Motor speed (rpm)
τ = Torque

3. Results and Discussion

The suggested design's findings are derived from the no-load and load analyses. The design is performed at no load circumstances such as cogging torque, back-emf, magnetic flux lines, and flux distribution, while the load analysis is performed in terms of torque, armature flux linkage, power, and speed.

3.1 Result of no-load test

3.1.1 Coil Test Analysis

The coil test analysis is done by setting the polarity of the PM flux in clockwise and anticlockwise directions to create north and south magnetic the twelve-coil test. The polarity and winding direction of the armature coil are set in a clockwise way, but the PM direction is set in a counterclockwise direction, creating 12 south and 12 north poles. Next, each slot containing a coil flux linkage is tested with the motor moving at 1,500 revolutions per minute. From the 12-coil test analysis, the four same waveforms will be simplified into a phase indicating each phase of a three-phase system.

After the 12-coil test, From the result of the 6 coils test, the same flux set for the coil. A combination of the same waveform flux will produce 3 flux patterns. From the 12-coil flux linkage

pattern, 4 of them will have the same identical pattern such as coil 1, coil 4, coil 7 and 10. After that, coil 2, coil 5, coil 8 and coil 11 while coil 3, coil 6, coil 9 and coil 12. From these results, it is possible to see the waveforms U, V and W.

The connection and coil link for U, V, and W coil test circuits must be in the proper connection for U, V, and W tests. The first combination that came out of the test using three different arrangements of coils groups the armature's coils 1, 4, 7, and 10 as armature coil 1 and is depicted as a V. The second combination is thus represented as U and is composed of the armature coils 2, 5, 8, and 11 acting as armature coil 2. The armature coils 3, 6, 9, and 12 are merged to form armature coil 3 for the opposite group, which is denoted by W. The flux of the three-phase flux linkage, denoted by U, V, and W, is shown in Figure 3.

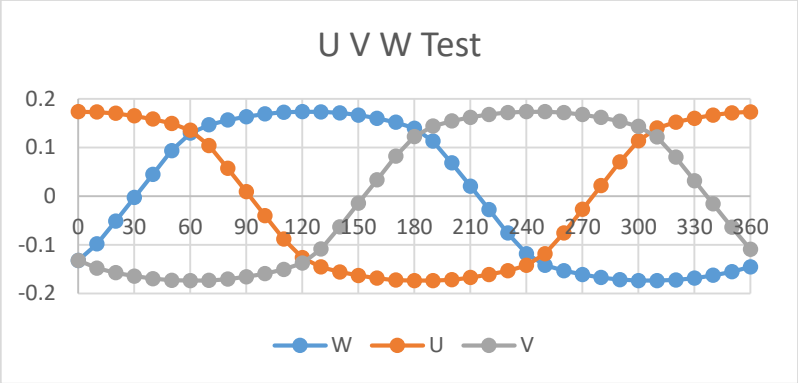

Figure 3: Flux linkage of Dual Rotor PMFSM U, V and W

3.2 Result of load test

To establish the flux features, the armature coil flux relationships were further analyzed at various armature current densities, Ja. Figure 4 and Figure 6 depict the relationship between the U-phase armature flux and the Ja range for the Double Rotor, while Figure 5 and Figure 7 depict the maximum U-phase flux in the Ja range. Identically when the value of Ja is 5, 10, 15, 20, 25, and 30 A_{rms}/mm^2, the graph is presented. It is clear in this figure that Ja will also increase when armature coil flux linkage is increased. The maximum value of U Phase flux linkage at various Ja is 0.531991 Wb.

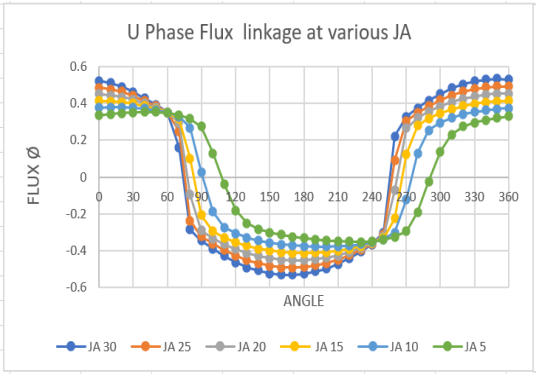

Figure 4: U-Phase flux linkage at various JA

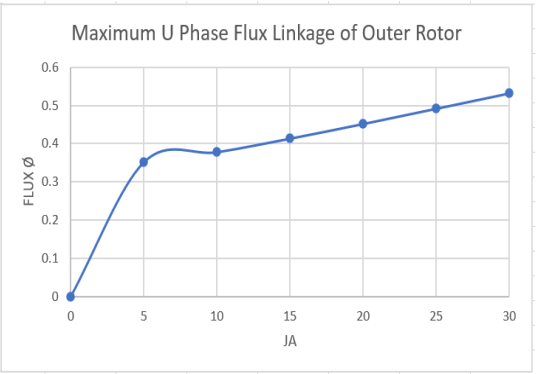

Figure 5: Maximum U Phase Flux Linkage of outer Rotor

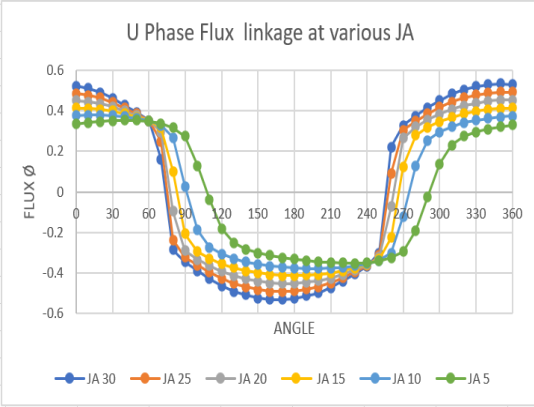

Figure 6: U-Phase flux linkage at various JA

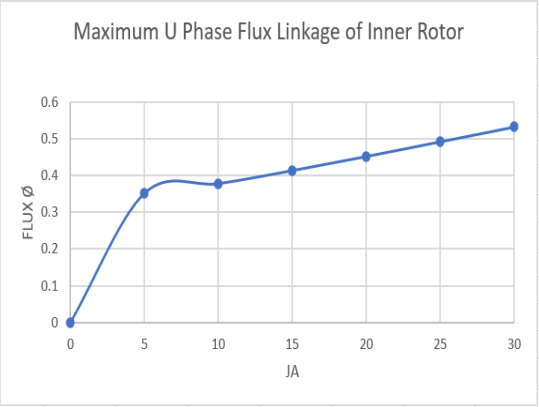

Figure 7: Maximum U Phase Flux Linkage of Inner Rotor

3.2.1 Torque Performance at Various Current Density Conditions

To confirm the patterns of torque variance when various current values were injected into the FEMM Coil motor at Double Rotor, torque at various Ja was analyzed. The Ja value of the armature current density is determined during the load test between 0 and 30 A_{rms}/mm^2 using Table 2 as a guide. Figure 8 displays the graph's torque and the Ja armature current density.

Figure 8 shows that the motor torque increases immediately as the current density of the Ja armature increases. The greater torque for the inner rotor in Figure 8 is 81.1454 Nm, while the greater torque for the outer rotor in Figure 8 is 97.42533 Nm. By comparing the two graphs, we can observe that the outer rotor torque value is higher than the inner rotor because of the outer rotor flux line's greater flux path coverage.

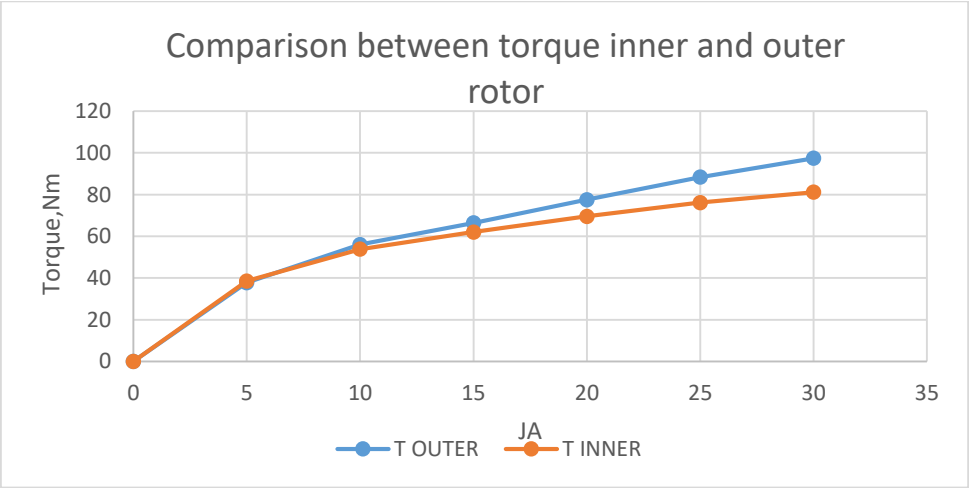

Figure 8: Comparison of Torque Inner and Outer Rotor

3.2.2 Torque and Power vs. Speed

After the torque is obtained, the speed and power are obtained at different armature current densities Ja. Figures 9 and 10 show the torque and power vs. speed for the outer and inner rotor of PMFSM. For the inner rotor and outer rotor, the maximum power obtained in which based on the graph the maximum power for inner rotor is 7.1960 KW and for the outer rotor the maximum power is 8.1323 KW. The speed and power are inverse to each other where when the speed increases the torque will decrease and as the speed increases the power will increase.

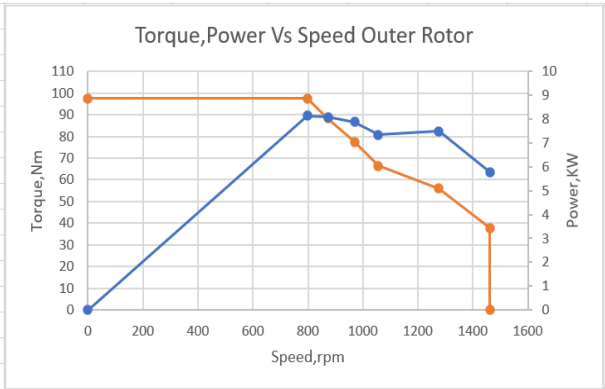

Figure 9: Torque and Power vs. Speed for outer rotor

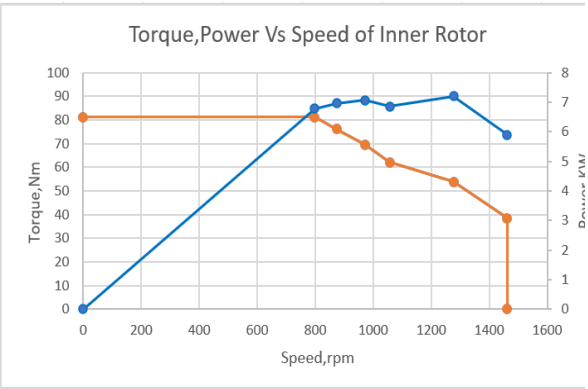

Figure 10: Torque and Power vs. Speed for inner rotor

3.2.3 Power Loss and Efficiency

Power loss and efficiency calculation to analyze the motor loss and efficiency because of copper loss in the armature coil and iron loss in the laminated core. Table 3 shows detailed losses in machine and efficiency.

Table 3: Detailed losses in machine and efficiency.

Point	**1**	**2**	**3**	**4**	**5**	**6**	**7**	**8**
Speed (rpm)	797.1	1461.7	200	200	200	600	600	600
Output Power (kW)	8132.3	5777.95	1675.52	1256.64	837.76	5026.55	3769.91	2513.27
Iron Loss (kW)	386.75	236.84	155.10	117.51	79.57	247.08	210.41	160.07
Copper Loss (kW)	2436.5	67.67	1083	327.58	97.48	1083	327.58	97.48
Efficiency %	74.23	94.9	57.51	73.84	82.55	79.08	87.51	90.71

4. Conclusion

The design and analysis of the double-rotor PMFSM are provided in this project. The design procedure has been thoroughly discussed. The magnetic flux linkages, cogging torque, induced voltage, and flux line distribution of a dual rotor PMFSM were investigated using a no-load analysis. To ensure that the machine operates in a three-phase system, a coil arrangement test was performed to determine the phase of each armature coil. The design process for the suggested machine has been extensively specified to proceed. The models were then put through a coil arrangement test to validate each stage of the armature coil and the operation of the equipment. For the no-load situation, the cogging torque, back-emf, flux line, and flux distribution of the suggested PMFSM design were examined. In addition, Load analysis was done to determine the performance in torque, power, and speed characteristics. However, the suggested dual rotor PMFSM exhibits drawbacks of complicated construction in comparison to the inner and outer rotor topologies. The result that has been obtained from the analysis is proven by the dual rotor PMFSM design better in terms of torque and output power. For no load and load analyses, the output performances of the proposed dual rotor PMFSM design and the manufactured dual rotor PMFSM design were also evaluated. As can be shown, this study's dual rotor PMFSM produced greater output torque performance (97.27 Nm for outer torque and 81.1454 Nm for inner torque) than those of the dual rotor PMFSMs used in previous studies, which generated 23.97 Nm for

outer torque and 18.36 Nm for inner torque. The power of both rotors eventually increased. The inner rotor's power increased from 1500 W to 7.1961 kW, while the outer rotor's power is raised from 1500 W to 8.1323 kW.

Acknowledgement

The authors would like to thank the Faculty of Electrical and Electronic Engineering, University Tun Hussein Onn Malaysia for its support.

References

[1] Ullah, W., Khan, F. and Hussain, S., 2022. Dual mechanical port power distribution in dual rotor permanent magnet flux switching generator for counter-rotating wind turbine applications.

[2] Analysis of Counter-Rotating Wind Turbines. (n.d.). ResearchGate. https://www.researchgate.net/publication/229050697_Analysis_of_Counter-Rotating_Wind_Turbines.

[3] Ullah, W., Khan, F., & Hussain, S. (2021). Investigation of Inner/Outer rotor permanent magnet flux switching generator for wind turbine applications. IEEE Access, 9, 149110–149117. https://doi.org/10.1109/ACCESS.2021.3122883.

[4] Ullah, W., Khan, F., & Umair, M. (2021). Optimal rotor poles and structure for the design of consequent pole permanent magnet flux switching machine. Chinese Journal of Electrical Engineering, 7(1), 118–127. https://doi.org/10.23919/CJEE.2021.00001155.